Lipids (2011) 46:991–1003
DOI 10.1007/s11745-011-3596-3

ORIGINAL ARTICLE

ApoB siRNA-induced Liver Steatosis is Resistant to Clearance by the Loss of Fatty Acid Transport Protein 5 (*Fatp5*)

Brandon Ason · Jose Castro-Perez · Samnang Tep · Alice Stefanni · Marija Tadin-Strapps · Thomas Roddy · Thomas Hankemeier · Brian Hubbard · Alan B. Sachs · W. Michael Flanagan · Nelly A. Kuklin · Lyndon J. Mitnaul

Received: 16 March 2011 / Accepted: 6 July 2011 / Published online: 9 August 2011

Abstract The association between hypercholesterolemia and elevated serum apolipoprotein B (APOB) has generated interest in APOB as a therapeutic target for patients at risk of developing cardiovascular disease. In the clinic, mipomersen, an antisense oligonucleotide (ASO) APOB inhibitor, was associated with a trend toward increased hepatic triglycerides, and liver steatosis remains a concern. We found that siRNA-mediated knockdown of *ApoB* led to elevated hepatic triglycerides and liver steatosis in mice engineered to exhibit a human-like lipid profile. Many genes required for fatty acid synthesis were reduced, suggesting that the observed elevation in hepatic triglycerides is maintained by the cell through fatty acid uptake as opposed to fatty acid synthesis. Fatty acid transport protein 5 (*Fatp5*/*Slc27a5*) is required for long chain fatty acid (LCFA) uptake and bile acid reconjugation by the liver. *Fatp5* knockout mice exhibited lower levels of hepatic triglycerides due to decreased fatty acid uptake, and shRNA-mediated knockdown of *Fatp5* protected mice from diet-induced liver steatosis. Here, we evaluated if siRNA-mediated knockdown of *Fatp5* was sufficient to alleviate *ApoB* knockdown-induced steatosis. We determined that, although *Fatp5* siRNA treatment was sufficient to increase the proportion of unconjugated bile acids 100-fold, consistent with FATP5's role in bile acid reconjugation, *Fatp5* knockdown failed to influence the degree, zonal distribution, or composition of the hepatic triglycerides that accumulated following *ApoB* siRNA treatment.

Keywords APOB · Liver steatosis · siRNA · FATP5 · Slc27a5 · siRNA combinations

Abbreviations

APOB	Apolipoprotein B
ASO	Antisense oligonucleotide
CLinDMA	2-{4-[(3b)-cholest-5-en-3-yloxy]-butoxy}-N,N-dimethyl-3-[(9Z,12Z)-octadeca-9,12-dien-1-yloxy]propan-1-amine
d	Deoxy
f	2′ fluoro
FATP5	Fatty acid transport protein 5
H & E	Hematoxylin and eosin
IHTG	Intra-hepatic triglyceride
LCFA	Long chain fatty acid uptake
LDL-c	LDL cholesterol
LNP	Lipid nanoparticle
MTP	Microsomal transfer protein
PEG-DMG	Monomethoxy(polyethyleneglycol)-1,2-dimyristoylglycerol

Brandon Ason and Jose Castro-Perez contributed equally.

Electronic supplementary material The online version of this article (doi:10.1007/s11745-011-3596-3) contains supplementary material, which is available to authorized users.

B. Ason · S. Tep · M. Tadin-Strapps · A. B. Sachs · W. Michael Flanagan · N. A. Kuklin
Sirna Therapeutics/Merck & Co. Inc., San Francisco, CA 94158, USA

B. Ason (✉)
Amgen Inc., 1120 Veterans Blvd, San Francisco, CA 94080, USA
e-mail: brandon.ason@amgen.com

J. Castro-Perez · A. Stefanni · T. Roddy · B. Hubbard · L. J. Mitnaul
Division of Cardiovascular Diseases and Atherosclerosis, Merck Research Laboratories, Rahway, NJ 07065, USA

J. Castro-Perez · T. Hankemeier
Division of Analytical Biosciences, LACDR, Leiden University, P.O. Box 9502, 2300 RA, Leiden, The Netherlands

siRNAs	Small interfering RNAs
TCA	Taurocholic acid
o	2′ O-methyl (o)
VLDL	Very low density lipoprotein

Introduction

Elevated LDL cholesterol (LDL-c) promotes atherosclerosis, and it is well established that reducing LDL-c helps to mitigate the risk of developing cardiovascular disease in patients with hypercholesterolemia [1–7]. LDL-c consists of a single apolipoprotein B-100 (APOB-100) molecule, cholesterol, cholesterol-esters and triacylglycerols that are comprised of various dietary and de novo synthesized fatty acids [8]. In the liver, APOB is required for very low density lipoprotein (VLDL) formation and serves as the scaffold to solubilize cholesterol and fatty acids (in the form of triglycerides) for secretion into the blood for circulation [8]. An association between hypercholesterolemia and increased APOB protein levels, together with the observation that reductions in *ApoB* synthesis reduce LDL-c and the incidence of atherosclerosis, has generated interest in APOB as a therapeutic target [9–13]. Both antisense oligonucleotides (ASOs) and small interfering RNAs (siRNAs) targeting *ApoB* reduce LDL-c in mice and in non-human primates [14–18]. In mice, *ApoB* ASOs reduced LDL-c without inducing hepatic steatosis, a liability of microsomal transfer protein (MTP) inhibitors that block triglyceride-rich lipoprotein assembly and secretion [19]. In patients, mipomersen, an *ApoB* targeting ASO, reduces both LDL-c and APOB, demonstrating the potential for an *ApoB*-targeted therapeutic [20–24]. Liver steatosis induced by inhibiting *ApoB*, however, remains an important concern. Recently, mipomersen administration at a sub-maximum efficacious dose was shown to be associated with a trend toward increased intra-hepatic triglyceride (IHTG) content for mipomersen-treated patients with one of the ten patients developing mild steatosis [20]. In addition, mice harboring a base-pair deletion in the coding region of *ApoB* (*ApoB-38.9*) exhibited hepatic triglyceride accumulation [25]. In order to attenuate the risk of liver steatosis associated with an *ApoB*-targeted therapeutic, one approach would be to combine an *ApoB* ASO or siRNA with another therapeutic that increases the clearance of hepatic triglycerides.

Fatty acid transport protein 5 (*Fatp5*/*Slc27a5*) mediates the uptake of long chain fatty acids (LCFAs) to the liver and is involved in bile acid reconjugation during enterohepatic recirculation [26, 27]. *Fatp5* knockout mice exhibit lower levels of hepatic triglycerides and free fatty acids due to decreased liver fatty acid uptake [27]. Furthermore, Doege et al. [25] recently showed that adenovirus-shRNA-mediated silencing of *Fatp5* mRNA not only protected mice from high fat diet-induced liver steatosis but also reversed steatosis once it was established. This suggested that a FATP5 inhibitor may be an attractive combination therapy with an APOB-targeted therapeutic.

Besides of its role in free fatty acid uptake, FATP5 also plays a critical role in reconjugation of bile acids during enterohepatic recirculation to the liver, and complete deletion of *Fatp5* resulted in a significant increase in unconjugated bile acids in both bile and serum [26]. Activation of FXR, a bile acid nuclear receptor, with bile acids or synthetic activators has been shown to reduce the secretion of triglyceride-rich VLDL from the liver in mice, which was associated with a decrease in *Srebp1* and *2* pathway genes [28]. The involvement of FATP5 in bile acid metabolism suggests that it too may play a role in hepatic triglyceride metabolism via FXR. However, the contributions of the bile acid reconjugation activity of FATP5 on hepatic steatosis or the contribution of FATP5 on APOB-induced steatosis are currently unknown. By utilizing two siRNAs specifically targeting *Fatp5* and *ApoB*, we evaluated the ability of *Fatp5* siRNA treatment to alleviate *ApoB* siRNA-induced liver steatosis.

Materials and Methods

siRNA Design

siRNAs were designed to the mRNA transcripts using a previously published design algorithm [34]. siRNA sequences contained the following chemical modifications added to the 2′ position of the ribose sugar when indicated: deoxy (d), 2′ fluoro (f), or 2′ O-methyl (o) [34]. Modification abbreviations are given immediately preceding the base to which they were applied. Passenger strands were capped with an inverted abasic nucleotide on the 5′ and 3′ ends. The control siRNA sequence (Cntrl siRNA) consists of:
iB;fluU;fluC;fluU;fluU;fluU;fluU;dA;dA;fluC;fluU;fluC;
fluU;fluC;fluU;fluU;fluC;dA;dG;dG;dT;dT;iB
passenger strand and
fluC;fluC;fluU;omeG;omeA;omeA;omeG;omeA;omeG;
omeA;omeG;fluU;fluU;omeA;omeA;omeA;rA;rG;rA;omeU;
omeU guide strand sequences.
The *Fatp5*(951) siRNA sequence consists of:
iB;fluC;fluU;dG;fluC;fluC;dA;fluU;dA;fluU;fluU;fluC;dA;
fluU;fluC;fluU;fluU;fluU;dA;fluC;dT;dT;iB
passenger strand and

rG;rU;rA;omeA;omeA;omeG;omeA;fluU;omeG;omeA;
omeA;fluU;omeA;fluU;omeG;omeG;fluC;omeA;omeG;
omeU;omeU guide strand sequences.
The *ApoB*(10168) siRNA sequence consists of:
iB;fluU;fluC;dA;fluU;fluC;dA;fluC;dA;fluC;fluU;dG;dA;
dA;fluU;dA;fluC;fluC;dA;dA;dT;dT;iB
passenger strand and
rU;rU;rG;omeG;fluU;omeA;fluU;fluU;fluC;omeA;omeG;
fluU;omeG;fluU;omeG;omeA;fluU;omeG;omeA;omeU;
omeU guide strand sequences.

siRNA Synthesis

siRNAs were synthesized by methods previously described [35]. For each siRNA, the two individual strands were synthesized separately using solid phase synthesis, and purified by ion-exchange chromatography. The complementary strands were annealed to form the duplex siRNA. The duplex was then ultrafiltered and lyophilized to form the dry siRNA. Duplex purity was monitored by LC/MS and tested for the presence of endotoxin by standard methods.

Preparation of siRNA-Lipid Nanoparticle (LNP) Complex

LNPs were made as described previously [36]. The encapsulation efficiency of the particles was determined using a SYBR Gold fluorescence assay in the absence and presence of triton, and the particle size measurements were performed using a Wyatt DynaPro plate reader. The siRNA and lipid concentrations in the LNP were quantified by a HPLC method, developed in house, using a PDA detector.

In Vivo siRNAs Treatments

All in vivo work was performed according to an approved animal protocol as set by the Institutional American Association for the Accreditation of Laboratory Animal Care. C57Bl/6 mice engineered to be hemizygous for a knockout of the LDL receptor and hemizygous for the overexpression of the human cholesterol ester transfer protein (CETP) driven by the endogenous apoA1 promoter within a C57Bl/6 background [B6-Ldlr<tm1>Tg(apoA1-CETP); Taconic] were used for these studies. Mice ~16–20 weeks of age were fed Lab Diets (5020 9F) starting 2 weeks prior to the start of the study. siRNAs were administered by intravenous (i.v.) injection. Animals were dosed on days 0 and 14 with either 3 mg/kg of a single LNP formulated siRNA or 1.5 mg/kg of two LNP formulated siRNAs for a 3 mg/kg total siRNA combination dose. For siRNA combinations, siRNA were formulated individually and hand-mixed immediately prior to injections. Animals were euthanized by CO_2 inhalation. Immediately after euthanasia, serum was collected using serum separator tubes and allowed to clot at room temperature for 30 min. Liver sections were excised, placed in either RNA Later (Qiagen) (right medial lobe), 10% buffered formalin (10% NBF, left medial lobe), or flash frozen (the remainder), and stored until further use.

RNA Isolation and qRT-PCR

RNA was isolated using an RNeasy96 Universal Tissue Kit (Qiagen) according to the supplied product protocol and as described previously [37]. TaqMan Gene Expression Assays (Applied Biosystems) were performed as described within the product protocol using the following primer probes, Mm00447768_m1 for *Fatp5*, Mm01545154_g1 for *ApoB*, and Cat# 4352339E for the reference, *Gapdh*. All reactions were performed in duplicate, and data were analyzed using the ddCt method with *Gapdh* serving as in [38]. Data represented as the $\log_2$-fold change (ddCt) relative to the control siRNA. For analysis of the selected *Srebp1c* and *Srebp2* pathway genes and *Scd1*, expression was normalized to an average of that of mouse *β-actin* (*Actb*), Glyceraldehyde 3-phosphate dehydrogenase (*Gapdh*), Beta-glucuronidase (*Gusb*), Hypoxanthine–guanine phosphoribosyltransferase (*Hprt1*), Peptidylprolyl isomerase A (*Cyclophilin A*/*Ppia*) and ribosomal protein 113a (*Rp113a*) in each sample. Expression levels of all genes analyzed were normalized to an average of the housekeeping genes (listed above) to obtain dCt. Fold regulation is calculated as: ddCt of gene in treatment group/dCt of gene in control group. Significance (p value) was calculated from a two-tailed t test between control and treatment groups. Accession numbers for the primer/probes used are listed in Supplemental Table 1.

Cholesterol and Triglyceride Analysis

Serum for cholesterol and triglyceride analysis was analyzed using Wako's total and HDL cholesterol kits according to the supplied product protocol and as described previously [37]. Non-HDL, which serves as an approximation for LDL, was calculated by subtracting HDL from total cholesterol measurements. The percent difference relative to the control siRNA was calculated using the following equation $\{100 \times [1-(\text{experimental/control})]\}$.

Histology and Hematology

Mouse livers were fixed with 10% neutral buffered formalin. One hepatic lobe was treated with osmium tetroxide solution, to visualize lipids, overnight at room temperature prior to paraffin embedding and processing. The other

hepatic lobe was embedded and processed in paraffin and hematoxylin and eosin (H&E) stained. Samples were sectioned at a thickness of 5 μm. The osmium-stained samples were digitalized using an Aperio ScanScope XT. Percent area (positive pixel count) was calculated using the positive pixel count algorithm (MAN-0024) supplied with the imaging software (Aperio). Samples were also reviewed by a board-certified veterinary pathologist and scored for inflammation and lipidosis using a semi-quantitative score.

Measurement of Serum APOB

The APOB levels in serum were measured by LC/MS as described previously [29]. The concentration of APOB peptide was calculated by dividing the area under the curve for the analyte by the area of its internal standard and multiplying by the internal standard concentration. The concentration of APOB was then converted to and reported as mg/dL.

LC/MS Sample Preparation and Analysis for Bile Acid Conjugation and Hepatic Triglycerides

Terminal bile samples from each group were collected using the stick and pull method. Samples were diluted 1:1,000 v/v in 50% acetonitrile + 0.1% formic acid/50% water + 0.1% formic acid, followed by the addition of 1 μM total internal standard solution (D_4-TCA, D_4-CA, D_4-GCA) (Sigma-Isotec, St. Louis, MO, USA). The mixture was vortexed for 10 s, centrifuged for 10 min at 15,000*g*, and then stored at −20 °C until LC/MS analysis. Supernatant was injected (10 μL) directly onto the LC/MS system.

A 50-mg slice of frozen liver from each animal was homogenized in 2-mL polypropylene tubes containing a 14-mm ceramic bead using a Precellys 24 homogenizer (Bertin Technologies, Montigny-le-Bretonneux, France). A non-naturally occurring internal standard solution (20 μL) containing TG 51:0 (Sigma Aldrich, St Louis, MO, USA) 0.8 mg/mL along with dichloromethane/methanol (2:1 v/v) was added to each sample prior to homogenization [39]. Samples were homogenized at 5,500 RPM, 2 × 30 s, with a 15 s pause between cycles. In order to generate a two layer liquid separation, 200 μL of distilled water was added, vortexed for 30 s, followed by centrifugation at 20,000*g* at 5 °C for 10 min. 10 μL of the lower layer, containing the lipids, was removed without disrupting the liver tissue homogenate disk. This was followed by dilution of the extracted lipid sample 1/50 in a solvent mixture (65% ACN, 30% IPA, 5% H_2O).

External endogenous calibration standards in buffer solution were used to cover the endogenous concentrations present in the bile and liver tissues. The inlet system was comprised of an Acquity UPLC (Waters, Milford, MA, USA). Bile and lipid extracts were injected (2 μL) onto a 1.8-μm particle 100 × 2.1 mm id Waters Acquity HSS T3 column (Waters). The column was maintained at 55 °C with a 0.4-mL/min flow rate for the lipid analysis and 65 °C with a 0.7-mL/min flow rate for the bile analysis. A binary gradient system was utilized for the analysis of both sample sets. Two different gradient conditions were used. For the lipid analysis, the same conditions were used as previously described [40]. For the bile acid analysis, water + 0.1% formic acid was used as eluent A. Eluent B consisted of acetonitrile + 0.1% formic acid (Burdick & Jackson, USA). A linear gradient (curve 6) was performed over a 13-min total run time. During the initial portion of the gradient, it was held at 80% A and 20% B. For the next 10 min, the gradient was ramped in a stepped linear fashion to 35% B (curve 5) in 4 min, 45% B in 7.5 min and 99% B in 9.5 min and held at this composition for 1.6 min. Hereafter, the system was switched back to 80% B and 20% A and equilibrated for an additional 2.9 min.

The inlet system described was directly coupled to a hybrid quadrupole orthogonal time of flight mass spectrometer (SYNAPT G2 HDMS; Waters MS Technologies, Manchester, UK). Electrospray (ESI) positive and negative ion ionization modes were used. In both ESI modes, a capillary voltage and cone voltage of ±2 kV and ±30 V, respectively, were used. The desolvation source conditions were as follows: for the desolvation gas 700 L/h was used and the desolvation temperature was kept at 450 °C. Data were acquired over the mass range of 50–1,200 Da.

The LC/MS data acquired was processed by the use of a quantitative data deconvolution package (Positive software by MassLynx; Waters, MA, USA). Data are presented as ± standard error of the mean (SEM). Differences between groups were computed by either Student's *t* test or by two-way ANOVA (GraphPad Prism, La Jolla, CA, USA). Post-test analysis for quantifiable variables was conducted using either Bonferroni or Mann–Whitney *U* non-parametric test with two-tailed *p* values. Values of $p < 0.05$ were considered statistically significant.

Lipid Nomenclature

The nomenclature utilized in this manuscript is in accordance with Lipidmaps (http://www.lipidmaps.org). In brief, a triglyceride described as TG 52:2 is interpreted as a triglyceride containing 52 carbons attached to the glycerol back-bone and two double bonds in the fatty acyl chain as described by Fahy et al. [41].

Results

Sustained Knockdown of Both ApoB and Fatp5 mRNA Transcripts was Achieved with siRNAs Administered Either Alone or in Combination

To investigate if we can simultaneously silence both *ApoB* and *Fatp5*, we administered siRNAs specifically targeting *ApoB* and *Fatp5*, alone and in combination, to CETP/LDLR hemizygous female mice (mice exhibiting a human-like lipid profile) fed a low-fat western diet. Changes to the lipid profile were obtained through a hemizygous mutation of the LDL receptor (±LDLR) and the hemizygous over-expression of a mouse apoA1 promoter-driven human CETP transgene (±apoA1-hCETP). This led to an elevation in LDL and a cholesterol profile that more closely resembled the HDL–LDL ratio observed in humans [29]. Female mice were fed a low-fat western diet ad libitum and treated with siRNAs formulated in a lipid nanoparticle (LNP) to achieve delivery to the liver [30]. Animals were dosed on days 0 and 14 with either 3 mg/kg of a single siRNA or 1.5 mg/kg of two siRNAs for a 3 mg/kg total siRNA combination dose. Efficacy was analyzed using qRT-PCR on liver samples collected on day 21. Analysis of mRNA expression levels revealed no appreciable difference in knockdown (KD) between *ApoB* siRNA treatments administered either alone or in combination with the *Fatp5* siRNA (Fig. 1a; ≥90% KD across all groups). Similar results were observed for the *Fatp5* siRNA, where ≥89% knockdown of *Fatp5* was observed (Fig. 1b).

Fatp5 Knockdown Impaired Bile Acid Reconjugation

The ratio of unconjugated/conjugated bile acid in the bile was used as a biological indicator for the loss of FATP5 activity following siRNA treatment to female mice fed a low-fat western diet ad libitum [26]. A significant increase in the proportion of unconjugated bile acids was observed for all *Fatp5* siRNA treatment groups, indicative of the loss of FATP5 activity (Fig. 2a; $p = 0.0003$, t test, Mann–Whitney post-test, cntrl siRNA groups vs. *Fatp5* siRNA groups). The unconjugated/conjugated ratio for the cntrl/cntrl siRNA group and the *Fatp5*/*Fatp5* siRNA group was 0.004 and 2.2, respectively. The ratio was lower for some of the *Fatp5* siRNA treatment groups when combined with the *ApoB* siRNA, but nevertheless exhibited a significant level of target engagement when compared with the control siRNA. Cholic acid in the *Fatp5* groups was the most predominant unconjugated bile acid found in bile (Fig. 2b), which showed a dramatic increase in concentration (0.77 mM in control siRNA vs. 77.95 mM in *Fatp5*) after knockdown of *Fatp5* ($p = 0.0003$, t test, Mann–Whitney post-test). Conjugated bile acids, specifically taurocholic acid (TCA), showed the reverse effect following *Fatp5* knockdown ($p = 0.1304$, t test, Mann–Whitney post-test). The levels of TCA decreased to 43.2 mM in comparison with the cntrl siRNA group 69.7 mM (data not shown). The ratio of unconjugated/conjugated bile acid in the serum reflected that of the bile, with a significant increase in the unconjugated levels (data not shown).

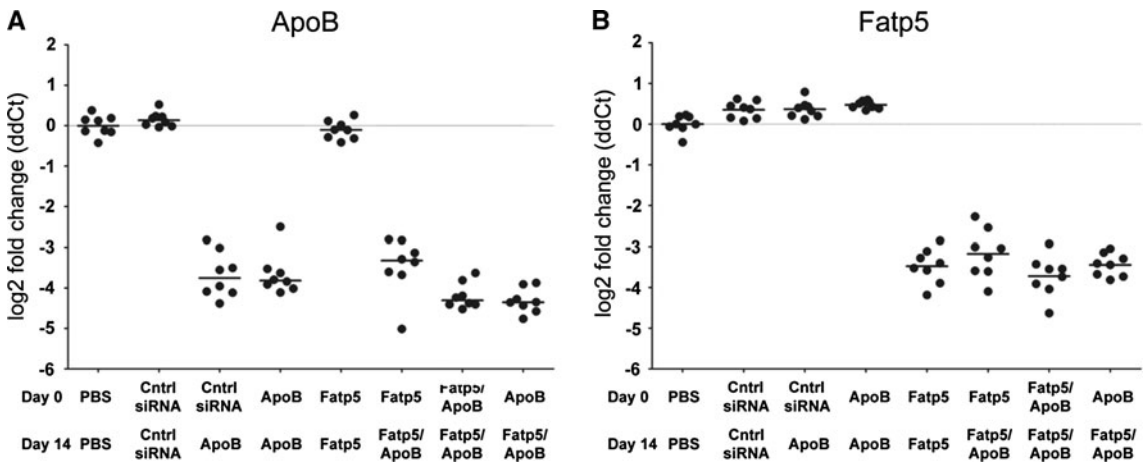

Fig. 1 Similar levels of *ApoB* and *Fatp5* mRNAs were observed for all groups containing siRNAs targeting these genes, either alone or in combination. Mice ($n = 8$/group) were treated with siRNAs targeting *ApoB* and *Fatp5* alone or in combination (*ApoB*, *Fatp5*, *Fatp5*/*ApoB*) at days 0 and 14. Gene expression was analyzed using qRT-PCR (TaqMan) on day 21 (**a**, **b**) post the initial dose. PBS and a control siRNA (*cntrl siRNA*) served as negative controls. Data represented as the log2 fold change (*ddCt*) relative to the cntrl siRNA treatment of individual animals (*circles*) and the group means (*bars*) are shown

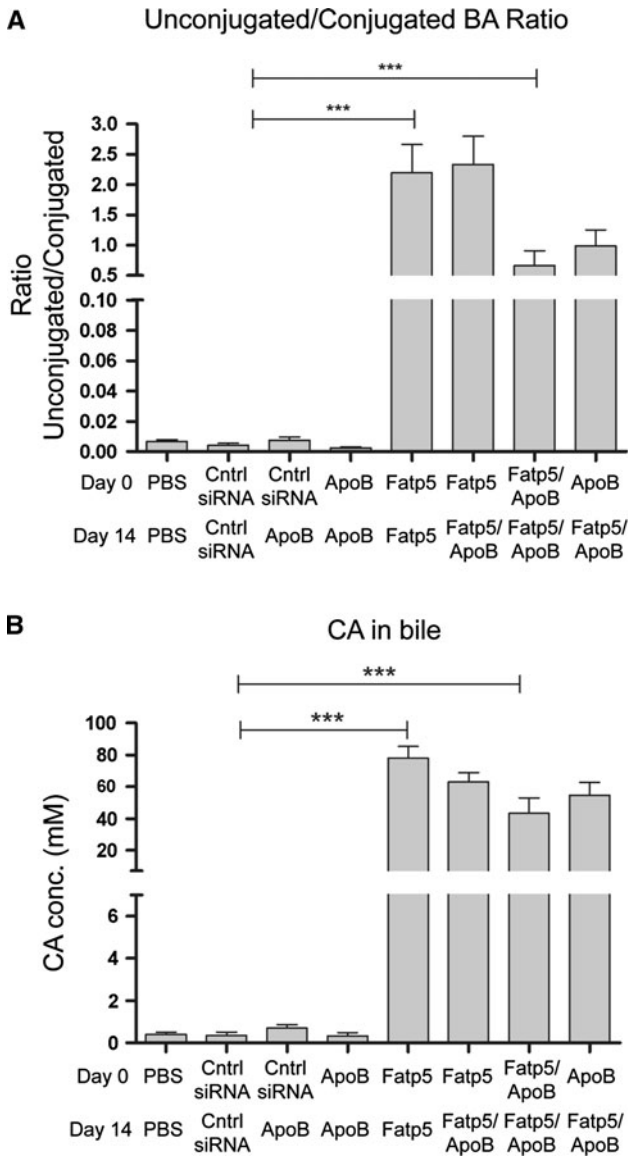

Fig. 2 *Fatp5* knockdown reduces bile acid (*BA*) reconjugation. **a** An increase in the level of unconjugated/conjugated bile acid ratio (***$p \leq 0.001$, *t* test, Mann–Whitney post-test) was observed following *Fatp5* knockdown. **b** Cholic acid (*CA*) concentrations exhibited an increase in the concentration measured (***$p \leq 0.001$, *t* test, Mann–Whitney post-test) by LC/MS after treatment with the *Fatp5* siRNA. Data represented as the group means (*bars*) ± SD ($n = 8$/group)

ApoB siRNA Treatment Led to Significant Reductions in Serum APOB Protein, Cholesterol and Triglyceride Levels Alone and in Combination with a Fatp5-Targeting siRNA

ApoB siRNA treatment, either alone or in combination with a siRNA targeting *Fatp5*, caused a significant reduction ($p \leq 0.001$) in serum APOB levels in female mice fed a low-fat western diet ad libitum (Fig. 3). APOB protein reductions were consistent with the reductions in hepatic

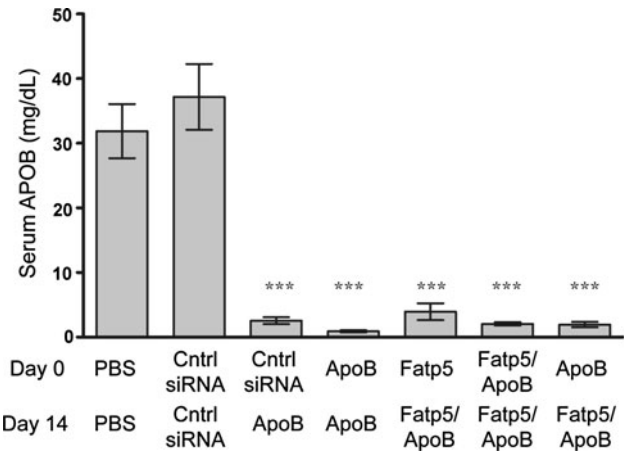

Fig. 3 Serum APOB protein levels were reduced following *ApoB* siRNA treatment. APOB levels in serum were measured by LC/MS on day 21 following days 0 and 14 doses as indicated on the *x*-axis. Data represented as the group means (*bars*) ± SD ($n = 8$/group). Significance (***$p \leq 0.0001$) relative to the siRNA control-treated group was calculated using a one-way ANOVA, Tukey post-test

ApoB mRNA levels (Fig 1a). This led to reductions in circulating cholesterol and triglyceride levels. On day 21, similar reductions in total (76–84%), HDL (67–78%), and non-HDL (79–90%) cholesterol were observed across all *ApoB* siRNA treatment groups (Fig. 4a–c). No significant decrease in cholesterol levels were observed for the *ApoB* + *Fatp5* siRNA combination group relative to the *ApoB* siRNA individual treatment group.

Serum triglycerides were also significantly reduced for *ApoB* siRNA treatments either alone or in combination on day 21 (Fig. 4d). Taken together, these data point to similar and significant changes in serum cholesterol across *ApoB* siRNA treatment groups that correlated with the observed reductions in *ApoB* mRNA and serum protein levels.

Fatp5 siRNA Treatment Failed to Alleviate ApoB siRNA-induced Liver Steatosis

To determine if *Fatp5* siRNA treatment was sufficient to alleviate *ApoB* siRNA-induced liver steatosis, liver sections were processed, sectioned, and stained with either osmium or H&E. Image analysis of the osmium stained slides revealed similar levels of significant lipid accumulation across all *ApoB* siRNA treatment groups relative to the PBS, *Fatp5*, or control siRNA groups (Fig. 5a, b). These data indicated that *Fatp5* siRNA treatment failed to alleviate *ApoB* siRNA-induced liver steatosis in female mice fed a low-fat western diet ad libitum. For the PBS, *Fatp5*, and control siRNA groups, there was some evidence of a periportal to midzonal (zones 1 and 2) distribution of lipid droplets within hepatocytes (Fig. 5b). This contrasted the lipid distribution following *ApoB* siRNA treatment,

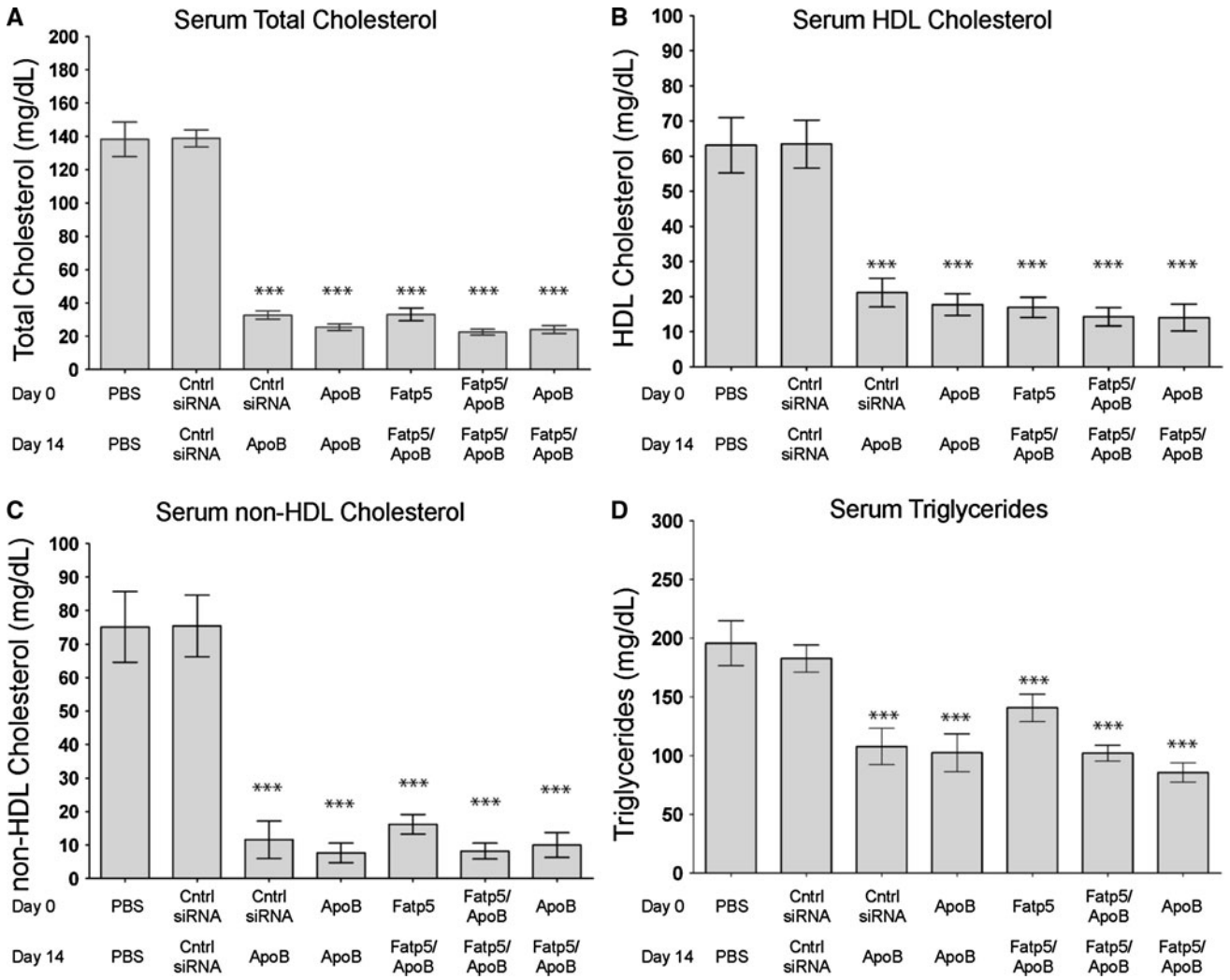

Fig. 4 Comparable levels of serum cholesterol and triglycerides were observed for *ApoB* siRNA treatments either alone or in combination with a siRNA-targeting *Fatp5*. Total cholesterol (**a**), HDL cholesterol (**b**), and triglycerides (**d**) were measured on day 21 following days 0 and 14 doses as indicated on the *x*-axis. Non-HDL cholesterol (**c**) was calculated by subtracting the HDL cholesterol value from the total cholesterol value. Data represented as group means (*bars*) ± SD ($n = 8$/group). The percent difference relative to the control siRNA is shown. Significance (***$p \leq 0.0001$) was calculated using a one-way ANOVA, Tukey post-test, and reported for treated groups relative to the siRNA control (*cntrl siRNA*) treatment

where diffuse infiltration (all zones) was observed (Fig. 5b). The *ApoB*-treated groups displayed lipid droplets that were smaller and more evenly distributed, while fewer but larger lipid droplets were observed for the remaining groups in many instances and as shown in Fig. 5b. By H&E staining, hepatocytes in the *ApoB* siRNA treatment groups appeared diffusely swollen, with granular to vacuolated cytoplasmic spaces (data not shown).

Fatp5 Knockdown Failed to Alter ApoB siRNA-induced Liver Triglyceride levels or Composition

Total triglyceride composition analysis by LC/MS revealed a significant increase in the level of triglycerides found in the liver following treatment with *ApoB* siRNA when compared with siRNA control (Fig. 6a; Cntrl siRNA 7.5 μg/mg of tissue vs. *ApoB* siRNA 35.5 μg/mg of tissue, $p = 0.0002$, *t* test with Mann–Whitney post-test). Comparative measurements between the *ApoB*/*ApoB* and the *Fatp5*/*Fatp5* + *ApoB* groups demonstrated that there was no protection from triglyceride accumulation in female mice fed a low-fat western diet ad libitum. LC/MS indicated that triglycerides 52:2 and 52:3 were significantly higher ($p \leq 0.0001$, two-way ANOVA with Bonferroni post-test) following *Fatp5*/*Fatp5* + *ApoB* treatment relative to *ApoB*/*ApoB* treatment (Fig. 6b). Triglycerides 52:4 and 54:3, although not statistically significant, also showed an increase in the *Fatp5*/*Fatp5* + *ApoB* cohort in

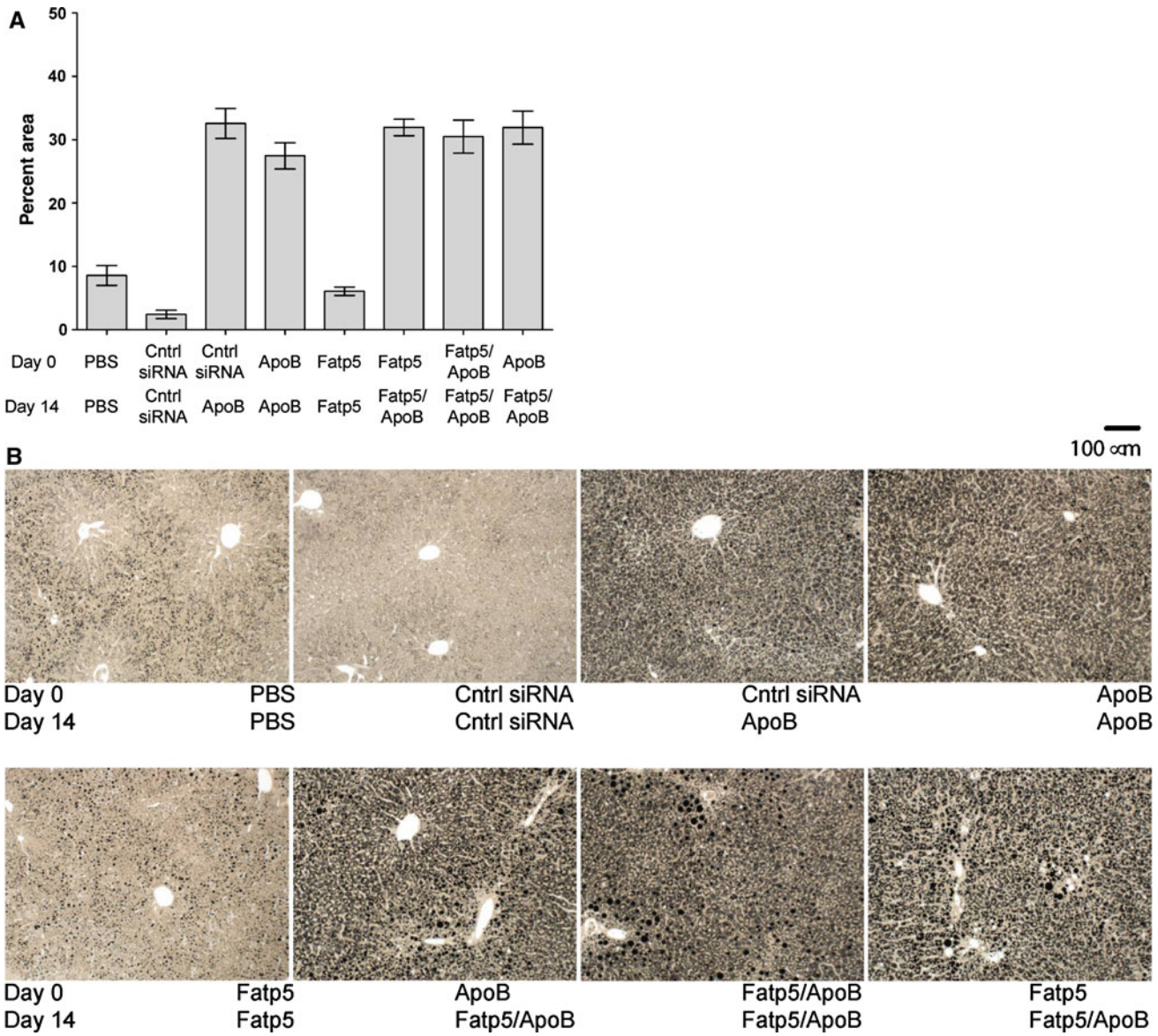

Fig. 5 Similar levels of liver steatosis were observed across all *ApoB* siRNA treatment groups. **a** Osmium-stained images were digitized and pixel intensities were quantitated for day 21. Data represented as the group mean ± SD ($n = 8$/group). **b** Images representative of each of the treatment groups are shown

comparison with the *ApoB*/*ApoB* cohort. Structure elucidation by collision-induced dissociation MS/MS provided information about the possible fatty acid composition for each triglyceride. Triglyceride 52:2 contained 16:0/18:1/18:1, triglyceride 52:3 contained 16:0/18:1/18:2, triglyceride 54:3 contained 18:1/18:1/18:1 and triglyceride 54:3 contained 18:1/18:2/18:1. These triglycerides were confirmed by accurate mass and the use of external standards (data not shown). All of these significantly relevant triglycerides have constituent fatty acids which are non-essential, suggesting that they may be derived from de novo synthesis.

The Hepatic Sterol Response Differed After ApoB and Fatp5 siRNA Treatments

To investigate the hepatic gene response to *ApoB*, *Fatp5* or combination treatments, we performed qRT-PCR analysis on genes involved in the sterol response element binding protein 1 and 2 pathways (*Srebp1* and *Srebp2*). Interestingly, although *ApoB* knockdown induced steatosis, it resulted in a significant decrease in many genes involved in both pathways (Table 1), including genes that are key regulators of fatty acid and triglyceride synthesis (*Fasn*, *Scd*, *Fads1/2*, *Acsl3/5*). As previously described, deletion

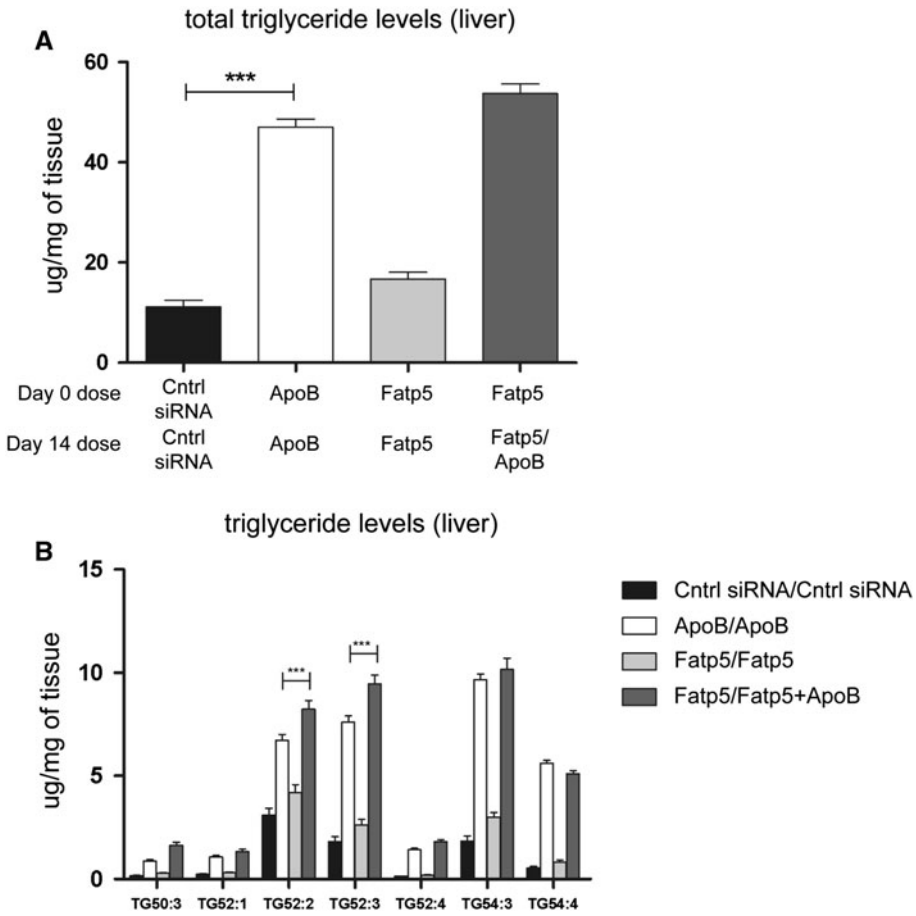

Fig. 6 *Fatp5* siRNA treatment fails to alter *ApoB* siRNA-induced liver triglyceride levels or composition. The total triglyceride pool size and composition was measured for different siRNA administrations (*Cntrl siRNA/Cntrl siRNA*, *ApoB/ApoB*, *Fatp5/Fatp5* and *Fatp5/Fatp5 + ApoB*). **a** A large increase in liver triglycerides was observed for the *ApoB/ApoB* group relative to the control siRNA (***$p = 0.0002$, *t* test with Mann–Whitney post-test). *Fatp5* siRNA treatment (*Fatp5/Fatp5 + ApoB*) did not show protection from *ApoB* siRNA-induced liver steatosis. **b** Specific triglycerides *TG 52:2* and *TG 52:3* showed an increase in their concentrations in both the *ApoB/ApoB* and *Fatp5/Fatp5 + ApoB* groups suggesting that *Fatp5* knockdown fails to alter the triglyceride composition induced by *ApoB* knockdown (***$p \leq 0.0001$, two-way ANOVA with Bonferroni post-test)

[31] or silencing [25] of *Fatp5* caused a reduced uptake of hepatic free fatty acids from serum, which caused a subsequent increase in genes involved in fatty acid synthesis. In contrast to *ApoB* siRNA treatment, Table 1 shows that *Fatp5* siRNA treatment resulted in a significant increase in both *Srebp1* and *Srebp2* pathways. Although bile acid conjugation levels changed and there was a significant increase in cholic acid in bile (Fig 3b), transcription of FXR or key regulators of FXR did not change (data not shown). *ApoB* siRNA treatment appeared to have a stronger effect on the *Srebp1/2* pathways than *Fatp5* siRNA since the simultaneous reductions of both resulted in a hepatic gene signature more similar to that of *ApoB* siRNA treatment alone.

Discussion

In this report, we found that siRNA-mediated knockdown of *ApoB* led to a significant reduction in serum lipids, including HDL, which was associated with an increase in hepatic triglycerides leading to liver steatosis in CETP/LDLR hemizygous mice (a mouse model having a human-like lipid profile). It is worth noting that similar results were observed on day 28 for all end points measured [mRNA knockdown, serum lipids, and histological analysis of hepatic lipid levels (data not shown)].

ApoB siRNA-mediated steatosis contrasts with results reported for ASO-mediated *ApoB* knockdown where only modest but not significant increases in hepatic triglycerides were observed following 6 weeks of biweekly (25 mg/kg) treatment that resolved by week 20 [14]. Crooke et al. reasoned that a compensatory mechanism, which included the activation of AMPK leading to increased fatty acid oxidation and the down-regulation of genes involved in fatty acid synthesis and transport, led to the resolution of hepatic triglyceride accumulation [14]. However, we also observed decreased gene expression within these pathways following the knockdown of *ApoB*. In addition, we observed increased serum ketone levels following *ApoB* siRNA treatment, which is indicative of increased fatty acid oxidation (data not shown). Furthermore, mice harboring a base-pair deletion in the coding region of *ApoB* (*ApoB-38.9*) also exhibited hepatic triglyceride accumulation and decreased expression of genes involved in fatty acid synthesis [25]. Taken together, these data suggest that an alternative mechanism may explain the lack of ASO-mediated steatosis and the discrepancy between *ApoB*

Table 1 *Srebp1c* and *Srebp2* gene expression changes observed following *ApoB*, *Fatp5,* and combination siRNA treatments

	Gene	ApoB		Fatp5		Fatp5/Fatp5 + ApoB	
		Fold regulation	*p* value	Fold regulation	*p* value	Fold regulation	*p* value
Srebp1c pathway	Acaca	–1.46	0.0705	1.78[a]	0.0156	–1.86[b]	0.0266
	Acacb	–1.69[b]	0.0084	1.61[a]	0.0070	–5.40[b]	0.0098
	Fasn	–2.99[b]	0.0026	2.05[a]	0.0203	–2.03	0.0830
	Scd	–3.62[b]	0.0009	1.95[a]	0.0007	–2.91[b]	0.0104
	Fads1	–2.18[b]	0.0000	1.13	0.0514	–2.18[b]	0.0000
	Fads2	–2.39[b]	0.0000	1.24	0.0705	–2.36[b]	0.0001
	Acsf2	1.36[a]	0.0075	1.12	0.0792	1.28[a]	0.0074
	Acsl1	1.19	0.1635	–1.18	0.3571	1.06	0.6852
	Acsl3	–2.16[b]	0.0002	1.05	0.8005	–1.76[b]	0.0202
	Acsl4	–1.24	0.1148	–1.10	0.3702	–1.25	0.0948
	Acsl5	–1.28[b]	0.0405	1.40[a]	0.0020	–1.40[b]	0.0475
Srebp2 pathway	Hmgcs1	–1.60[b]	0.0238	1.93[a]	0.0020	–1.24	0.3368
	Hmgcr	–2.23[b]	0.0034	1.72	0.0740	–1.30	0.5900
	Mvk	–1.11	0.3513	1.51[a]	0.0086	–1.02	0.8580
	Pmvk	–2.30[b]	0.0004	1.52[a]	0.0068	–2.33[b]	0.0033
	Mvd	–3.26[b]	0.0033	1.94[a]	0.0072	–1.98	0.0528
	Idi1	–1.63[b]	0.0212	1.99[a]	0.0017	–1.24	0.3330
	Fdps	–2.60[b]	0.0022	1.88[a]	0.0039	–2.20[b]	0.0237
	Fdft1	–1.43[b]	0.0095	1.72[a]	0.0011	–1.10	0.6770
	Cyp51a1	–1.75[b]	0.0058	1.81[a]	0.0010	–1.40	0.1238
	Dhcr7	–1.65[b]	0.0065	1.65[a]	0.0007	–1.54	0.1193

Selected *Srebp1* and *Srebp2* pathway genes were analyzed after siRNA treatments. Mice were treated with siRNAs targeting *ApoB* and *Fatp5* alone or in combination (*ApoB*, *Fatp5*, *Fatp5*/*ApoB*) at days 0 and 14. Gene expression was analyzed using qRT-PCR (TaqMan) on day 21. Fold regulation was calculated for the treatment group relative to the control siRNA group.

[a] Indicates a significant induction ($p \leq 0.05$) and [b]a significant reduction ($p \leq 0.05$) in expression relative to the control siRNA group. Significance (*p* value) was calculated using a two-tailed *t* test between control and treatment groups

siRNA and ASO treatments, which could be explained, at least in part, by the fact that we are observing slightly greater *ApoB* knockdown (~90 vs. ~75%) and cholesterol lowering [~80 (non-HDL) vs. 66% (LDL)] relative to the ASO-mediated changes.

From our results, HDL appears lower and serum triglycerides higher than one would initially expect for *ApoB* knockdown. While the cause of the decrease in HDL following *ApoB* siRNA treatment is unknown, it is likely that the HDL components provided by APOB-containing particles are reduced following *ApoB* knockdown leading to a reduction HDL levels, which is consistent with findings by Tadin-Strapps et al. [29, 31]. In addition, while serum triglycerides appear disproportionately higher relative to serum APOB for *ApoB* siRNA-treated groups (Fig. 3 relative to Fig. 4d), some of this apparent discrepancy could be due to the production of larger, more triglyceride-rich, non-HDL particles for the limited number of particles produced. It also remains likely that serum triglycerides are artificially elevated relative to other endpoints, since serum triglycerides are measured enzymatically and glycerol is a reaction intermediate. Thus, any glycerol within the serum would lead to a higher reading than would otherwise be expected.

Fatty acids are either transported into the liver or synthesized de novo. Since fatty acids are required for triglyceride synthesis and *ApoB* knockdown reduced the expression of many of the genes involved in de novo hepatic fatty acid synthesis, we rationalized that liver steatosis induced by *ApoB* knockdown could be maintained, at least in part, by the accumulation of fatty acids taken up by hepatocytes [29]. FATP5 is a transporter of long chain fatty acids (LCFAs) into hepatocytes [27, 32], and we reasoned that reducing LCFA uptake by knocking-down *Fatp5* would reduce hepatic triglyceride levels induced by *ApoB* knockdown. We found that *Fatp5* knockdown does not influence the size, composition, or zonal distribution of the hepatic triglyceride pool generated by *ApoB* siRNA treatment. Lipid levels for the *Fatp5* siRNA treatment alone were too low to reliably assess differences in the hepatic triglyceride population relative to the control siRNA group, although results reported by Doege et al. [27] would

suggest that reductions in FATP5 would disproportionately decrease the saturated and polyunsaturated fatty acid containing triglycerides relative to monounsaturated fatty acid containing triglycerides.

It remains possible that FATP5 may not function as a transporter of fatty acids under our conditions. In the studies reported here, animals were fed a chow diet containing 9% fat ad libitum, whereas *Fatp5* knockout mice fed a similar diet (a chow diet containing 5% fat) exhibited the most dramatic changes in hepatic lipid accumulation under prolonged fasting conditions [32]. One could also argue that *Fatp5* knockdown may induce the expression of other *Fatp* family members, which could compensate for the loss of FATP5 activity under our conditions. However, this is unlikely, since *Fatp5* knockout mice did not exhibit altered expression of *Fatp1-4* or *Fatp6* [32], and we did not observe a change in the expression of either of the two *Fatps* evaluated (*Fatp2* or *Fatp4*, data not shown). Alternatively, both *Fatp2* and *Fatp5* are highly expressed in liver, and *Fatp2* knockdown has also been reported to decrease hepatic fatty acid uptake in mice [33]. Therefore, it remains possible that FATP2 is sufficient to mediate hepatic fatty acid uptake in the absence of FATP5 under our conditions.

Even though *Fatp5* knockdown failed to influence the hepatic triglyceride pool generated following *ApoB* knockdown, it did lead to a 100-fold increase in ratio of unconjugated to conjugated bile acids. The magnitude of the shift within the bile acid pool, from predominately conjugated to predominately unconjugated bile acids, is consistent with FATP5 being required for the majority of bile acid reconjugation during enterohepatic recirculation. Our results are inline with the results reported for *Fatp5* knockout mice and suggest that *Fatp5* siRNA treatment is sufficient to influence FATP5 activity [26]. We expect these changes to have only a minor effect on fat absorption, since, consistent with Hubbard et al. [26], we observed that unconjugated bile acids are found within gall bladder bile. Thus, unconjugated bile acids can be efficiently secreted into bile following *Fatp5* knockdown and should therefore be available for fat absorption. *Fatp5* knockout mice also exhibited secondary metabolic changes leading to decreased food intake. Although, it is unclear if this is due to altered bile acid metabolism via the inhibition of bile acid reconjugation, altered lipid metabolism via the inhibition of fatty acid uptake, or both. While outside the scope of this work, it remains possible to use siRNAs targeting *Fatp5* to address this question, since we observed the inhibition of bile acid reconjugation but not fatty acid uptake under these conditions.

Finally, we have shown that *Fatp5* knockdown resulted in a significant increase in genes involved in hepatic cholesterol biosynthesis (*Srebp2* pathway) and fatty acid synthesis (*Srebp1* pathway). This is consistent with the increase in fatty acid synthase expression and defects in bile acid reconjugation reported for the loss of FATP5 activity [26, 27].

One could, therefore, speculate that changes in bile acid conjugation levels would result in an increase in de novo cholesterol synthesis, requiring more acetyl-CoA, which may promote fatty acid synthesis.

Acknowledgments We would like to thank Duncan Brown for siRNA design, Dipali Ruhela and her group for providing the LNP formulations, Jing Kang and Natalya Dubinina for their help with the 'in-life' portion of these studies, Carla S. Colon and David McLaren for their help with metabolite profiling, Wu Yin for help with the gene expression analysis, Kenny K. Wong, Steven R. Bartz, and Anthony K. Ogawa for helpful discussions, as well as Premier Laboratory for histological services and support with pathology review.

References

1. Steinberg D (2004) Thematic review series: the pathogenesis of atherosclerosis—an interpretive history of the cholesterol controversy: part I. J Lipid Res 45:1583–1593. doi:10.1194/jlr.R400003-JLR200
2. Steinberg D (2005) Thematic review series: the pathogenesis of atherosclerosis—an interpretive history of the cholesterol controversy: part II: the early evidence linking hypercholesterolemia to coronary disease in humans. J Lipid Res 46:179–190. doi:10.1194/jlr.R400012-JLR200
3. Steinberg D (2005) Thematic review series: the pathogenesis of atherosclerosis: an interpretive history of the cholesterol controversy, part III: mechanistically defining the role of hyperlipidemia. J Lipid Res 46:2037–2051
4. Steinberg D (2006) Thematic review series: The Pathogenesis of Atherosclerosis. An interpretive history of the cholesterol controversy, part V: The discovery of the statins and the end of the controversy. J Lipid Res 47:1339–1351. doi:10.1194/jlr.R600009-JLR200
5. Davis RA, Hui TY (2001) 2000 George Lyman Duff Memorial Lecture: atherosclerosis is a liver disease of the heart. Arterioscler Thromb Vasc Biol 21:887–898
6. Skalen K, Gustafsson M, Rydberg EK, Hulten LM, Wiklund O, Innerarity TL, Boren J (2002) Subendothelial retention of atherogenic lipoproteins in early atherosclerosis. Nature 417:750–754
7. Hulthe J, Fagerberg B (2002) Circulating oxidized LDL is associated with subclinical atherosclerosis development and inflammatory cytokines (AIR Study). Arterioscler Thromb Vasc Biol 22:1162–1167
8. Davidson NO, Shelness GS (2000) Apolipoprotein B: mRNA editing, lipoprotein assembly, and presecretory degradation. Annu Rev Nutr 20:169–193
9. Gaffney D, Forster L, Caslake MJ, Bedford D, Stewart JP, Stewart G, Wieringa G, Dominiczak M, Miller JP, Packard CJ (2002) Comparison of apolipoprotein B metabolism in familial defective apolipoprotein B and heterogeneous familial hypercholesterolemia. Atherosclerosis 162:33–43

10. Veerkamp MJ, de Graaf J, Bredie SJ, Hendriks JC, Demacker PN, Stalenhoef AF (2002) Diagnosis of familial combined hyperlipidemia based on lipid phenotype expression in 32 families: results of a 5-year follow-up study. Arterioscler Thromb Vasc Biol 22:274–282
11. Tybjaerg-Hansen A, Steffensen R, Meinertz H, Schnohr P, Nordestgaard BG (1998) Association of mutations in the apolipoprotein B gene with hypercholesterolemia and the risk of ischemic heart disease. N Engl J Med 338:1577–1584
12. Boren J, Lee I, Zhu W, Arnold K, Taylor S, Innerarity TL (1998) Identification of the low density lipoprotein receptor-binding site in apolipoprotein B100 and the modulation of its binding activity by the carboxyl terminus in familial defective apo-B100. J Clin Invest 101:1084–1093
13. Innerarity T, Mahley R, Weisgraber K, Bersot T, Krauss R, Vega G, Grundy S, Friedl W, Davignon J, McCarthy B (1990) Familial defective apolipoprotein B-100: a mutation of apolipoprotein B that causes hypercholesterolemia. J Lipid Res 31:1337–1349
14. Crooke RM, Graham MJ, Lemonidis KM, Whipple CP, Koo S, Perera RJ (2005) An apolipoprotein B antisense oligonucleotide lowers LDL cholesterol in hyperlipidemic mice without causing hepatic steatosis. J Lipid Res 46:872–884
15. Rozema DB, Lewis DL, Wakefield DH, Wong SC, Klein JJ, Roesch PL, Bertin SL, Reppen TW, Chu Q, Blokhin AV et al (2007) Dynamic PolyConjugates for targeted in vivo delivery of siRNA to hepatocytes. Proc Natl Acad Sci USA 104:12982–12987. doi:10.1073/pnas.0703778104
16. Zimmermann TS, Lee AC, Akinc A, Bramlage B, Bumcrot D, Fedoruk MN, Harborth J, Heyes JA, Jeffs LB, John M et al (2006) RNAi-mediated gene silencing in non-human primates. Nature 441:111–114
17. Soutschek J, Akinc A, Bramlage B, Charisse K, Constien R, Donoghue M, Elbashir S, Geick A, Hadwiger P, Harborth J et al (2004) Therapeutic silencing of an endogenous gene by systemic administration of modified siRNAs. Nature 432:173–178
18. Merki E, Graham MJ, Mullick AE, Miller ER, Crooke RM, Pitas RE, Witztum JL, Tsimikas S (2008) Antisense oligonucleotide directed to human apolipoprotein B-100 reduces lipoprotein(a) levels and oxidized phospholipids on human apolipoprotein B-100 particles in lipoprotein(a) transgenic mice. Circulation 118:743–753
19. Chandler CE, Wilder DE, Pettini JL, Savoy YE, Petras SF, Chang G, Vincent J, Harwood HJ Jr (2003) CP-346086: an MTP inhibitor that lowers plasma cholesterol and triglycerides in experimental animals and in humans. J Lipid Res 44:1887–1901
20. Visser ME, Akdim F, Tribble DL, Nederveen AJ, Kwoh TJ, Kastelein JJ, Trip MD, Stroes ES Effect of apolipoprotein-B synthesis inhibition on liver triglyceride content in patients with familial hypercholesterolemia. J Lipid Res 51:1057-1062
21. Akdim F, Visser ME, Tribble DL, Baker BF, Stroes ES, Yu R, Flaim JD, Su J, Stein EA, Kastelein JJ Effect of mipomersen, an apolipoprotein B synthesis inhibitor, on low-density lipoprotein cholesterol in patients with familial hypercholesterolemia. Am J Cardiol 105:1413-1419
22. Akdim F, Stroes ES, Sijbrands EJ, Tribble DL, Trip MD, Jukema JW, Flaim JD, Su J, Yu R, Baker BF et al (2010) Efficacy and safety of mipomersen, an antisense inhibitor of apolipoprotein B, in hypercholesterolemic subjects receiving stable statin therapy. J Am Coll Cardiol 55:1611–1618
23. Raal FJ, Santos RD, Blom DJ, Marais AD, Charng MJ, Cromwell WC, Lachmann RH, Gaudet D, Tan JL, Chasan-Taber S et al (2010) Mipomersen, an apolipoprotein B synthesis inhibitor, for lowering of LDL cholesterol concentrations in patients with homozygous familial hypercholesterolaemia: a randomised, double-blind, placebo-controlled trial. Lancet 375:998–1006
24. Kastelein JJ, Wedel MK, Baker BF, Su J, Bradley JD, Yu RZ, Chuang E, Graham MJ, Crooke RM (2006) Potent reduction of apolipoprotein B and low-density lipoprotein cholesterol by short-term administration of an antisense inhibitor of apolipoprotein B. Circulation 114:1729–1735
25. Lin X, Schonfeld G, Yue P, Chen Z (2002) Hepatic fatty acid synthesis is suppressed in mice with fatty livers due to targeted apolipoprotein B38.9 mutation. Arterioscler Thromb Vasc Biol 22:476–482
26. Hubbard B, Doege H, Punreddy S, Wu H, Huang X, Kaushik VK, Mozell RL, Byrnes JJ, Stricker-Krongrad A, Chou CJ et al (2006) Mice deleted for fatty acid transport protein 5 have defective bile acid conjugation and are protected from obesity. Gastroenterology 130:1259–1269
27. Doege H, Grimm D, Falcon A, Tsang B, Storm TA, Xu H, Ortegon AM, Kazantzis M, Kay MA, Stahl A (2008) Silencing of hepatic fatty acid transporter protein 5 in vivo reverses diet-induced non-alcoholic fatty liver disease and improves hyperglycemia. J Biol Chem 283:22186–22192
28. Mencarelli A, Renga B, Distrutti E, Fiorucci S (2009) Antiatherosclerotic effect of farnesoid X receptor. Am J Physiol Heart Circ Physiol 296:H272–H281
29. Tadin-Strapps M, Peterson LB, Cumiskey AM, Rosa RL, Mendoza VH, Castro-Perez J, Puig O, Zhang L, Strapps WR, Yendluri S et al. (2011) siRNA induced liver ApoB knockdown lowers serum LDL-cholesterol in a mouse model with human-like serum lipids. J Lipid Res 52:1084–1097
30. Morrissey DV, Lockridge JA, Shaw L, Blanchard K, Jensen K, Breen W, Hartsough K, Machemer L, Radka S, Jadhav V et al (2005) Potent and persistent in vivo anti-HBV activity of chemically modified siRNAs. Nat Biotechnol 23:1002–1007
31. Lieu HD, Withycombe SK, Walker Q, Rong JX, Walzem RL, Wong JS, Hamilton RL, Fisher EA, Young SG (2003) Eliminating atherogenesis in mice by switching off hepatic lipoprotein secretion. Circulation 107:1315–1321
32. Doege H, Baillie RA, Ortegon AM, Tsang B, Wu Q, Punreddy S, Hirsch D, Watson N, Gimeno RE, Stahl A (2006) Targeted deletion of FATP5 reveals multiple functions in liver metabolism: alterations in hepatic lipid homeostasis. Gastroenterology 130:1245–1258
33. Falcon A, Doege H, Fluitt A, Tsang B, Watson N, Kay MA, Stahl A (2010) FATP2 is a hepatic fatty acid transporter and peroxisomal very long-chain acyl-CoA synthetase. Am J Physiol Endocrinol Metab 299:E384–E393
34. Majercak J, Ray WJ, Espeseth A, Simon A, Shi XP, Wolffe C, Getty K, Marine S, Stec E, Ferrer M et al (2006) LRRTM3 promotes processing of amyloid-precursor protein by BACE1 and is a positional candidate gene for late-onset Alzheimer's disease. Proc Natl Acad Sci USA 103:17967–17972
35. Wincott F, DiRenzo A, Shaffer C, Grimm S, Tracz D, Workman C, Sweedler D, Gonzalez C, Scaringe S, Usman N (1995) Synthesis, deprotection, analysis and purification of RNA and ribozymes. Nucleic Acids Res 23:2677–2684
36. Abrams MT, Koser ML, Seitzer J, Williams SC, DiPietro MA, Wang W, Shaw AW, Mao X, Jadhav V, Davide JP et al (2010) Evaluation of efficacy, biodistribution, and inflammation for a potent siRNA nanoparticle: effect of dexamethasone co-treatment. Mol Ther 18:171–180
37. Ason B, Tep S, Davis HR Jr, Xu Y, Tetzloff G, Galinski B, Soriano F, Dubinina N, Zhu L, Stefanni A et al (2011) Improved efficacy for ezetimibe and rosuvastatin by attenuating the induction of PCSK9. J Lipid Res 52:679–687
38. Livak KJ, Schmittgen TD (2001) Analysis of relative gene expression data using real-time quantitative PCR and the 2(-delta delta C(T)) method. Methods 25:402–408

39. Bligh EG, Dyer WJ (1959) A rapid method of total lipid extraction and purification. Can J Biochem Physiol 37:911–917
40. Castro-Perez J, Previs SF, McLaren DG, Shah V, Herath K, Bhat G, Johns DG, Wang SP, Mitnaul L, Jensen K et al (2011) In vivo D_2O labeling to quantify static and dynamic changes in cholesterol and cholesterol esters by high resolution LC/MS. J Lipid Res 52:159–169
41. Fahy E, Subramaniam S, Murphy RC, Nishijima M, Raetz CR, Shimizu T, Spener F, van Meer G, Wakelam MJ, Dennis EA (2009) Update of the LIPID MAPS comprehensive classification system for lipids. J Lipid Res 50(Suppl):S9–S14